

# DeReCo: Decoupling Representation and Coordination Learning for Object-Adaptive Decentralized Multi-Robot Cooperative Transport

Kazuki Shibata<sup>1\*</sup>, Ryosuke Sota<sup>1\*</sup>, Shandil Dhiresch Bosch<sup>1,2\*</sup>,  
Yuki Kadokawa<sup>1</sup>, Tsurumine Yoshihisa<sup>1</sup>, and Takamitsu Matsubara<sup>1</sup>

**Abstract**—Generalizing decentralized multi-robot cooperative transport across objects with diverse shapes and physical properties remains a fundamental challenge. Under decentralized execution, two key challenges arise: object-dependent representation learning under partial observability and coordination learning in multi-agent reinforcement learning (MARL) under non-stationarity. A typical approach jointly optimizes object-dependent representations and coordinated policies in an end-to-end manner while randomizing object shapes and physical properties during training. However, this joint optimization tightly couples representation and coordination learning, introducing bidirectional interference: inaccurate representations under partial observability destabilize coordination learning, while non-stationarity in MARL further degrades representation learning, resulting in sample-inefficient training. To address this structural coupling, we propose DeReCo, a novel MARL framework that decouples representation and coordination learning for object-adaptive multi-robot cooperative transport, improving sample efficiency and generalization across objects and transport scenarios. DeReCo adopts a three-stage training strategy: (1) centralized coordination learning with privileged object information, (2) reconstruction of object-dependent representations from local observations, and (3) progressive removal of privileged information for decentralized execution. This decoupling mitigates interference between representation and coordination learning and enables stable and sample-efficient training. Experimental results show that DeReCo outperforms baselines in simulation on three training objects, generalizes to six unseen objects with varying masses and friction coefficients, and achieves superior performance on two unseen objects in real-robot experiments. The demonstration video is available at link.

## I. INTRODUCTION

This study considers decentralized multi-robot cooperative transport scenarios, where robots transport an object to a goal position using only local observations at execution time. These local observations exclude other robots' observations as well as privileged information about object-dependent properties such as shape, mass, and friction. Recent studies [1]–[7] adopt multi-agent reinforcement learning (MARL) to enable cooperative transport without relying on explicit dynamics models. However, most of these studies are evaluated in single-object settings and are not applicable to cooperative transport across objects with varying shapes and physical properties, particularly unseen objects not included

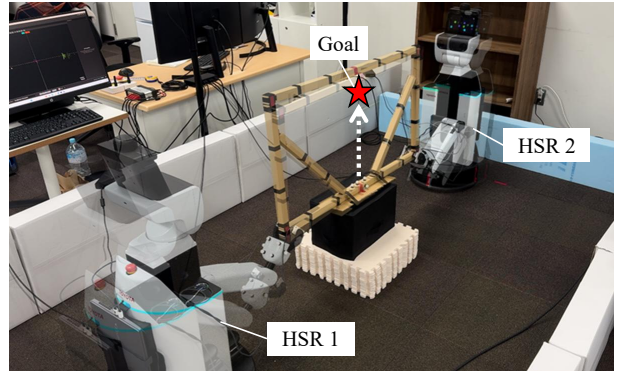
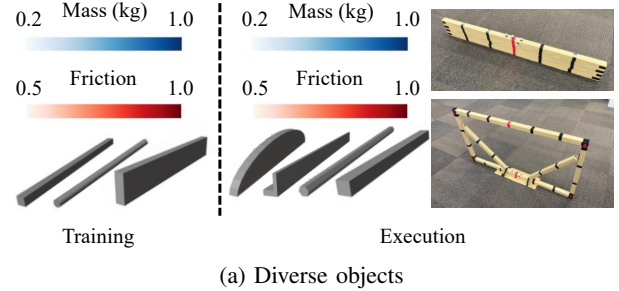


Fig. 1: Multi-robot cooperative transport of diverse objects using two HSRs.

during training. These limitations highlight the need for MARL approaches that generalize across diverse objects under decentralized execution.

Generalizing decentralized multi-robot cooperative transport across diverse objects poses two key challenges. First, object generalization under local observations constitutes a partial observability problem. If the environment state is defined to include object-dependent properties such as shape, mass, and friction, these properties are not directly observable at execution time. Robots must therefore infer object-dependent representations from limited sensory inputs. Second, cooperative transport inherently requires coordination among multiple robots. In MARL, coordination learning is affected by non-stationarity because each agent's policy evolves during training, making the environment non-stationary from the perspective of the other agents [8].

A typical approach jointly optimizes object-dependent representation and coordinated policies in an end-to-end manner while randomizing object shapes and physical properties. This joint optimization tightly couples representation and

\*These authors contributed equally to this work.

<sup>1</sup>All the authors are with the Division of Information Science, Graduate School of Science and Technology, Nara Institute of Science and Technology (NAIST), Nara, Japan.

<sup>2</sup>Shandil Dhiresch Bosch is with the Department of Cognitive Robotics, Faculty of Mechanical Engineering, Delft University of Technology, Delft, Netherlands.

coordination learning, introducing bidirectional interference: inaccurate representations under partial observability destabilize coordination, while MARL non-stationarity further degrades representation learning, resulting in sample-inefficient and unstable training.

To address this structural coupling, we decouple object-dependent representation learning under partial observability from coordination learning in MARL. Based on this design principle, we propose DeReCo, a novel MARL framework that decouples representation and coordination learning for object-adaptive multi-robot cooperative transport, improving sample efficiency and robust generalization across objects and transport scenarios. DeReCo adopts a three-stage training strategy: (1) centralized coordination learning with privileged object information, (2) reconstruction of object-dependent representations from local observations, and (3) progressive removal of privileged information for decentralized execution. This decoupling mitigates representation–coordination coupling and enables stable and sample-efficient learning.

The effectiveness of DeReCo is confirmed through cooperative transport experiments with two Human Support Robots (HSRs) in simulation and on real robot experiments, as shown in Fig. 1. In simulation, we trained policies using three object shapes with different masses and friction coefficients and confirmed that DeReCo improve training performance compared to several baselines. We then evaluated generalization on six unseen object shapes that were not included during training, showing that the proposed method maintains high success rates on unseen objects. We further demonstrate superior performance over the strongest baseline in hardware experiments using two unseen objects.

The main contributions of this work are as follows:

- We propose DeReCo, a novel MARL framework that decouples representation learning and coordination learning for object-adaptive decentralized multi-robot cooperative transport.
- We demonstrate through simulation that DeReCo consistently outperforms baseline methods across nine object shapes with varying masses and friction coefficients, including six shapes not included during training.
- We evaluate the effectiveness of DeReCo on real HSRs and show superior performance over the strongest baseline on two unseen objects.

## II. RELATED WORK

### A. Model-based Multi-robot Cooperative Transport

Model-based approaches to multi-robot cooperative transport assume an explicit object dynamics model and design controllers to drive the object state toward a desired target. Prior work has leveraged model-based optimization, including constrained optimal control [9]–[11] and MPC [12], [13]. To enable real-time control under limited communication bandwidth and computational resources, consensus-based distributed optimization and distributed nonlinear MPC have also been studied [14], [15]. As an alternative to

optimization-based formulations, decentralized adaptive control has been explored, with Lyapunov-based stability analysis providing convergence guarantees under uncertain object parameters [16]–[18].

Model-based formulations for cooperative transport offer stability and convergence guarantees, but they typically assume a rigid attachment between each robot’s grasp point and the object in the underlying dynamics. Our model-free method dispenses with explicit dynamics and remains effective when this rigid-contact assumption does not hold.

### B. MARL-based Multi-robot Cooperative Transport

Several studies have demonstrated that model-free MARL can enable cooperative transport on a wide range of robots, from mobile manipulators [1] and quadrupeds [2] to bipeds [3], [4] and aerial platforms with cable-suspended payloads [5].

A widely used MARL design is centralized training with decentralized execution (CTDE), which exploits global information during training to mitigate non-stationarity while executing decentralized policies from local observations. Scalability across varying team sizes has also been studied via consensus-based estimation [6] and curriculum learning with knowledge distillation [7].

Despite these advances, most existing methods are evaluated in single-object settings and are not applicable to cooperative transport across diverse objects. In contrast, our approach decouples object-dependent representation learning under partial observability from coordination learning under MARL non-stationarity, enabling decentralized cooperative transport across diverse objects.

### C. RL-based Transport of Diverse Objects

Several studies have adopted RL-based approaches to achieve generalization in object transport. A typical approach employs domain randomization over object shapes and physical properties and jointly optimizes object-dependent representations and policy learning in an end-to-end manner [19]–[21]. Another line of work adopts a multi-stage learning framework that separates object-dependent representation learning from policy learning [22]. Specifically, a policy is first trained with privileged object information; then an encoder is trained to reconstruct object-dependent representations from sensory inputs; finally, the policy is retrained using the reconstructed representations without privileged information.

Although prior work [22] separates representation learning from policy learning, it focuses on generalization in single-robot object transport and is not directly applicable to multi-robot settings. In contrast, our study decouples representation learning under partial observability from coordination learning in MARL under non-stationarity, enabling decentralized cooperative transport across diverse objects.

## III. PRELIMINARY

### A. Problem Setting

This study considers cooperative transport with two mobile manipulators, where the robots grasp and transport objects

with diverse shapes and physical properties. The control objective is to grasp an object and transport it to a specified goal pose in three-dimensional space.

Following [1], we make the following assumptions:

- Each robot can observe the position and orientation of its end-effector and the object.
- The other robot’s grasping pose and contact forces are not available to each robot.

Moreover, we make the following assumption:

- The object’s shape and physical properties are available during training, but are not accessible during execution.

This assumption is reasonable because this information is available in simulation during training, but is commonly unavailable in the real world.

### B. Decentralized Partially Observable Markov Decision Process (Dec-POMDP)

We formulate the cooperative transport problem as a Dec-POMDP [23]. It is defined by the tuple  $\langle \mathcal{S}, \mathcal{B}, \{\mathcal{A}^i\}_{i \in \mathcal{B}}, P, \{r^i\}_{i \in \mathcal{B}}, \{\mathcal{O}^i\}_{i \in \mathcal{B}}, \gamma \rangle$ , where  $s \in \mathcal{S}$  denotes the global state and  $\mathcal{B} := \{1, \dots, n\}$  is the set of robots. Robot  $i \in \mathcal{B}$  observes  $o_t^i$  and selects  $a_t^i$  at time  $t$ , and the actions of the  $n$  robots form  $a_t = (a_t^1, \dots, a_t^n)$ . Given  $(s_t, a_t)$ , the next state  $s_{t+1}$  is sampled from  $P(s_{t+1} | s_t, a_t)$ , and robot  $i$  receives a reward  $r_t^i$ .

The learning objective is to maximize the expected discounted return across the  $n$  robots, defined as  $J = \mathbb{E}[\sum_{i=1}^n R_t^i]$ , where  $R_t^i = \sum_{k=0}^{\infty} \gamma^k r_{t+k}^i$  denotes the discounted return of robot  $i$ .

### C. Multi-Agent Proximal Policy Optimization (MAPPO)

MAPPO [24] adopts an actor–critic algorithm in the CTDE setting. The critic is trained with access to the global state, whereas at execution each robot follows a decentralized policy conditioned only on its local observations. The critic is parameterized by  $\phi$  and outputs the state-value estimate  $V_\phi(s_t)$ . The actor of robot  $i$  is parameterized by  $\theta_i$  and defined as  $\pi_{\theta_i}(a_t^i | o_t^i)$ .

In MAPPO, each robot’s policy is optimized with the clipped surrogate objective:

$$\mathcal{L}_{\text{actor}}(\theta_i) = \mathbb{E}_t \left[ \min \left( \rho_t^i A_t, \text{clip}(\rho_t^i, 1 - \epsilon, 1 + \epsilon) A_t \right) \right], \quad (1)$$

where  $A_t$  represents the estimated advantage obtained via generalized advantage estimation (GAE) [25]. Here, The probability ratio  $\rho_t^i$  is defined as the ratio of the current policy to the previous one:  $\rho_t^i = \pi_{\theta_i}(a_t^i | o_t^i) / \pi_{\theta_i^{\text{old}}}(a_t^i | o_t^i)$ .

In addition, the critic is optimized with a clipped value loss:

$$\mathcal{L}_{\text{critic}}(\phi) = \mathbb{E}_t \left[ \max \left( (V_\phi(s_t) - \hat{R}_t)^2, (\text{clip}(V_\phi(s_t), V_\phi^{\text{old}}(s_t) - \epsilon, V_\phi^{\text{old}}(s_t) + \epsilon) - \hat{R}_t)^2 \right) \right], \quad (2)$$

where  $\hat{R}_t := \frac{1}{n} \sum_{i=1}^n R_t^i$ ,  $\epsilon > 0$  specifies the clipping range and  $V_\phi^{\text{old}}$  denotes the pre-update value estimate.

## IV. METHOD

### A. Overview of DeReCo

This section introduces DeReCo, a MARL framework for object-adaptive decentralized multi-robot cooperative transport. Fig. 2 illustrates the overall structure of the proposed framework.

DeReCo adopts a three-stage training strategy: (1) centralized coordination learning with privileged information, (2) reconstruction of object-dependent representations from local observations, and (3) progressive removal of privileged information for decentralized execution. This decoupling mitigates interference between representation and coordination learning and enables stable and sample-efficient training.

The training procedure of DeReCo is as follows:

- **Stage 1: MARL with privileged object information.** We learn coordination policies under centralized training using object-dependent representations from privileged object information, establishing stable coordination.
- **Stage 2: Adaptive encoder learning.** We learn an adaptive encoder that reconstructs object-dependent representations from local observations, enabling decentralized inference without privileged information.
- **Stage 3: MARL with adaptive encoder.** We retrain the coordination policies under CTDE using the adaptive encoder, enabling decentralized execution from local observations.

### B. Stage 1: MARL with Privileged Object Information

We first perform centralized training with privileged information to stabilize coordination learning under MARL non-stationarity. By providing reliable object-dependent representations during training, this stage avoids interference from representation learning under partial observability and establishes stable coordination policies.

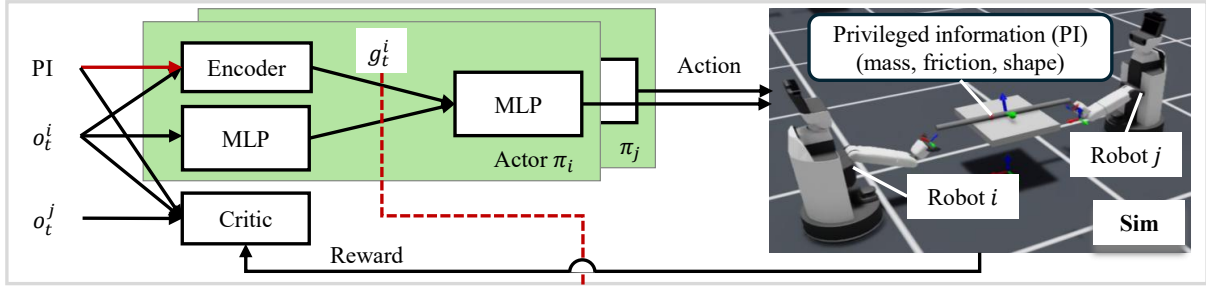
During centralized training, the critic leverages joint observations and privileged object information  $(o_t^i, o_t^j, p)$  to mitigate non-stationarity and is optimized by minimizing  $\mathcal{L}_{\text{critic}}$  to estimate the centralized value function. Here,  $o_t^i$  and  $o_t^j$  denote the local observations of robots  $i$  and  $j$  at time step  $t$ , and  $p$  denotes privileged object information. The actor  $\pi_\theta^i(a_t^i | o_t^i, p)$  is trained using the local observation and privileged information  $(o_t^i, p)$  to learn coordination policies and is optimized by minimizing  $\mathcal{L}_{\text{actor}}$ .

### C. Stage 2: Adaptive Encoder Learning

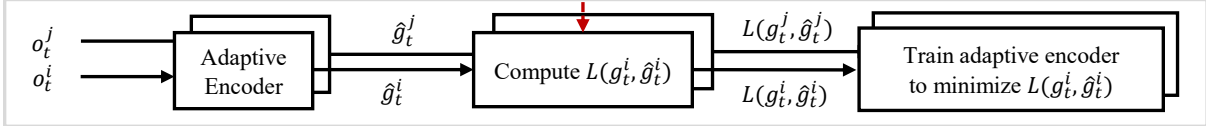
Privileged object information used in centralized training is not available under decentralized execution. To decouple object-dependent representation learning under partial observability from coordination learning in MARL, Stage 2 independently learns object-dependent representations from local observations via supervised learning. Specifically, Stage 2 consists of data collection and supervised training of the adaptive encoder.

**Data collection:** We generate diverse objects by sampling discrete shape types from a predefined one-hot-encoded set

Stage 1: MARL with privileged object information



Stage 2: Learning adaptive encoder



Stage 3: MARL with adaptive encoder

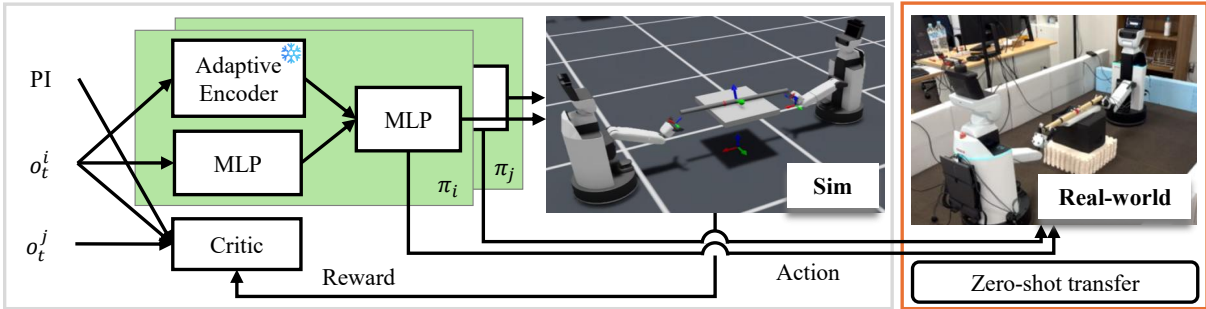


Fig. 2: Overview of the DeReCo for object-adaptive decentralized multi-robot cooperative transport

and sampling continuous physical properties uniformly from specified ranges. For each sampled object, we roll out the policy from Stage 1 and record pairs  $(o_t^i, g_t^i)$  for each robot  $i$ , where  $g_t^i$  is the object-dependent representation computed during rollouts using the encoder in Stage 1, as shown in Fig. 2. The representations  $g_t^i$  serve as supervision targets for training the adaptive encoder.

**Supervised learning of the adaptive encoder:** Under decentralized execution, each robot must infer object-dependent representations from its local observations without privileged object information. We therefore train an adaptive encoder  $e_\psi$  that reconstructs object-dependent representations as  $\hat{g}_t^i = e_\psi(o_t^i)$ , where  $\psi$  denotes the encoder parameters.

The adaptive encoder is trained in a supervised manner using target representations  $g_t^i$  collected in Stage 1. We optimize  $\psi$  by minimizing  $\mathcal{L}(g_t^i, \hat{g}_t^i)$ , defined as the mean squared error between the reconstructed representations  $\hat{g}_t^i$  and the targets  $g_t^i$ .

#### D. Stage 3: MARL with Adaptive Encoder

To enable decentralized execution without privileged object information, we progressively remove privileged information while maintaining coordinated behaviors. After establishing stable coordination through centralized training and independently learning object-dependent representations in Stage 2, we retrain the policy using the adaptive encoder.

Under the CTDE framework, the actor and critic are initialized from the Stage 1 weights and retrained. The

adaptive encoder learned in Stage 2 is frozen and used in the actor to reconstruct object-dependent representations from local observations. The critic leverages joint observations and privileged object information  $(o_t^i, o_t^j, p)$  during training to mitigate non-stationarity and is optimized by minimizing  $\mathcal{L}_{\text{critic}}$ . The actor  $\pi_\theta^i(a_t^i | o_t^i)$  is trained using local observation  $o_t^i$  to learn coordination policies and is optimized by minimizing  $\mathcal{L}_{\text{actor}}$ .

At execution time, each robot selects actions using only its local observation. By progressively removing privileged object information during training, this stage yields coordination policies for decentralized execution and enables stable and sample-efficient learning.

## V. EXPERIMENT

To assess the effectiveness of DeReCo, we conduct a cooperative transport experiment with two HSRs. This experiment aims to answer the following research questions:

- **RQ1:** Can DeReCo improve training performance? (Section V-B)
- **RQ2:** Does DeReCo generalize to diverse objects with different shapes and physical properties? (Section V-C)
- **RQ3:** Can the trained policy successfully transport unseen objects training in the real world? (Section V-D)

### A. Experimental Setup

1) **Simulation Setup:** The simulations were conducted using Isaac Sim, an NVIDIA physics simulator. The control

objective is for two HSRs to grasp and transport an object toward a goal position. Training was performed by running 512 parallel simulation environments in Isaac Sim.

The local observation of robot  $i$  is defined as  $o^i = [a_{t-1}^i, o_{\text{arm}}^i, o_{\text{grip}}^i, o_{\text{goal}}^i, o_{\text{obj}}^i, o_{\text{force}}^i] \in \mathbb{R}^{27}$ , where  $a_{t-1}^i \in \mathbb{R}^6$  is the previous action,  $o_{\text{arm}}^i \in \mathbb{R}^3$  the arm joint angles,  $o_{\text{grip}}^i \in \mathbb{R}^2$  the binary open/close states of the two gripper fingers,  $o_{\text{goal}}^i \in \mathbb{R}^3$  the distance vector to the goal,  $o_{\text{obj}}^i \in \mathbb{R}^7$  the object position and orientation relative to the end-effector, and  $o_{\text{force}}^i \in \mathbb{R}^6$  the ternary force signals from two triaxial sensors on the gripper fingers, obtained by discretizing the force change between consecutive steps into  $\{-1, 0, +1\}$  following [1]. The action is  $a^i = [a_{\text{base}}^i, a_{\text{arm}}^i, a_{\text{grip}}^i] \in \mathbb{R}^6$ , where  $a_{\text{base}}^i \in \mathbb{R}^2$  and  $a_{\text{arm}}^i \in \mathbb{R}^3$  denote planar base and arm joint velocity commands, respectively, and  $a_{\text{grip}}^i \in \mathbb{R}$  applies a torque to the gripper fingers. We use the same reward design as in [1].

At the beginning of each episode, the object is placed at the center of the table. The table height is sampled uniformly from  $[0.3, 0.6]$  m above the ground, and the goal position is fixed at a height of 0.8 m.

Furthermore, we evaluate performance using the success rate, where an episode is considered successful if the Euclidean distance between the object and the goal at the end of the episode is less than 0.1 m.

2) **Compared Methods:** To evaluate the proposed method, we compare it with the following MARL baselines:

- **MAPPO w/o PI:** A MAPPO trained without privileged information (PI), using only local observations, in an end-to-end manner.
- **MAPPO w/o PI + LSTM:** A recurrent variant of **MAPPO w/o PI**, where an LSTM is integrated into the encoder to infer object-dependent representations.
- **MAPPO w/o AE:** A MAPPO trained without the adaptive encoder (AE) in an end-to-end manner. The critic is trained with privileged information, local observations, and other robots' observations, whereas the actor is trained only from local observations.
- **MAPPO w/o AE + LSTM:** A recurrent variant of **MAPPO w/o AE**, where an LSTM is integrated into the encoder to infer object-dependent representations.
- **MAPPO w PI:** A MAPPO trained with both privileged information and local observations in an end-to-end manner.

3) **Network Architecture:** The network architectures used in each stage of the proposed method are designed as follows.

**Stage 1:** The actor and critic share the same network architecture. Privileged information and local observations are processed by an encoder, which is a fully connected (FC) layer. Local observations are also passed through another FC layer. The outputs of the encoder and the FC layer are concatenated and then passed through two additional FC layers. Each FC layer has 128 units with ReLU activation in the hidden layers. The output layer uses a linear activation for the critic and a tanh activation for the actor.

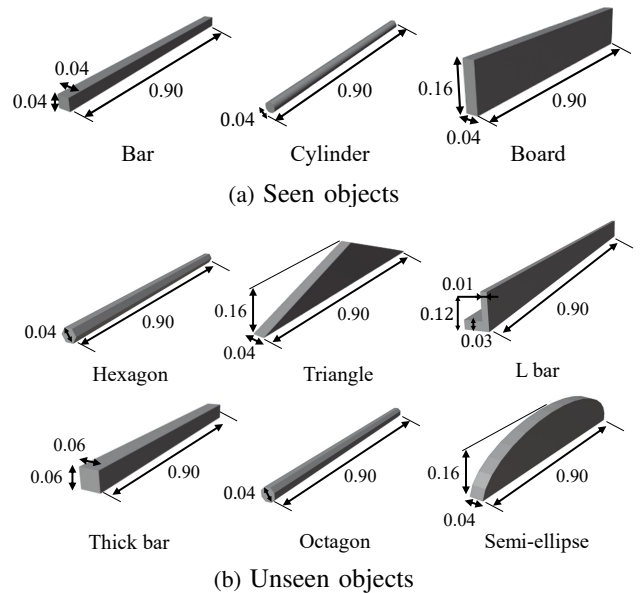


Fig. 3: Objects used in the simulation. All units are meters.

**Stage 2:** Following [22], the adaptive encoder is implemented as an LSTM. Specifically, we use a single-layer LSTM with 128 units.

**Stage 3:** The critic adopts the same network architecture as in Stage 1. The actor also follows the Stage-1 architecture, except that the encoder is replaced with the adaptive encoder. The actor and critic networks are initialized with the trained weights from Stage 1 and are then fine-tuned in Stage 3.

### B. RQ1: Can DeReCo Improve Training Performance?

1) **Setup:** To evaluate the effectiveness of DeReCo, we prepared a set of objects with different shapes and physical properties. During training, three object shapes were used, with masses ranging from 0.2 kg to 1.0 kg and friction coefficients ranging from 0.5 to 1.0. The objects used for training are shown in Fig. 3a. Training was performed for 50,000 steps, where each step corresponded to one policy action. For both the proposed and compared methods, training was conducted five times with different random seeds, using an identical seed set across all methods to ensure a fair comparison.

2) **Result:** Figure 4 compares the tracking reward during training. For **DeReCo**, we show the learning curve of Stage 3, since Stage 1 is identical to **MAPPO w PI** and is omitted to avoid redundancy. **MAPPO w PI** achieves higher tracking rewards than **MAPPO w/o PI**, indicating that privileged object information stabilizes coordination learning under MARL non-stationarity. However, jointly optimizing object-dependent representations and coordination policies in an end-to-end manner remains unstable, as observed in **MAPPO w/o AE**. In contrast, **DeReCo** achieves higher rewards than **MAPPO w/o AE**, demonstrating that decoupling representation learning from coordination learning mitigates representation–coordination interference during training. The recurrent baselines, **MAPPO w/o PI + LSTM** and **MAPPO**

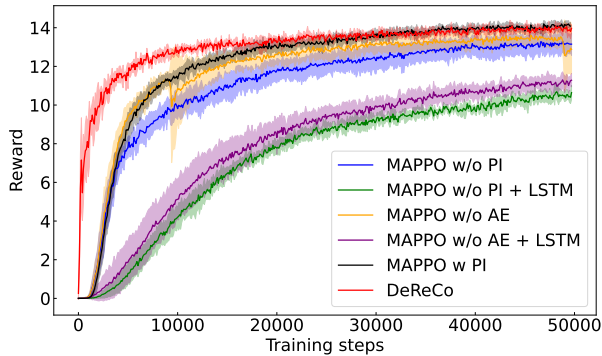


Fig. 4: Comparisons of the tracking reward

**w/o AE + LSTM**, exhibit lower rewards, suggesting that simply introducing recurrence into end-to-end training does not resolve the structural coupling between representation learning and coordination learning.

Overall, DeReCo can improve training performance by decoupling representation and coordination learning.

### C. RQ2: Does DeReCo Generalize to Diverse Objects with Different Shapes and Physical Properties?

1) **Setup:** We evaluate the policies on the three seen objects and six unseen objects with shapes not included in training, as shown in Fig. 3b. The object mass and friction coefficients are randomized within the same ranges as in training. All results are averaged over five independently trained policies, and each policy is evaluated for 1,000 trials using random seeds different from those used during training. We include **MAPPO w PI** as a reference, since it leverages privileged information at execution time. Because object IDs for unseen objects are not defined, we provide a random one-hot vector when evaluating **MAPPO w PI** on unseen objects.

2) **Result:** Table I presents the per-object and average success rates on the seen and unseen objects. On the seen objects, **DeReCo** outperforms **MAPPO w/o PI** and achieves performance comparable to **MAPPO w PI** across objects with different shapes. This indicates that **DeReCo** achieves high coordination performance by inferring object-dependent representations from local observations.

On unseen objects, **DeReCo** consistently outperforms **MAPPO w/o PI**, demonstrating improved generalization to novel shapes. **DeReCo** also surpasses **MAPPO w/o AE**, suggesting that reconstructing object-dependent representations from local observations is important for generalization when object shapes are not observed during training. In contrast, **MAPPO w/o PI + LSTM** and **MAPPO w/o AE + LSTM** underperform **DeReCo**, indicating that jointly learning object representations and coordination end-to-end with LSTM remains insufficient; explicitly reconstructing object-dependent representations leads to better generalization.

We further analyze failures on unseen objects for four representative methods as shown in Fig. 5. Failures are categorized into three types: (i) grasp-and-lift failures, where the robots cannot grasp and lift the object; (ii) post-lift drop

failures, where the object is dropped after lifting; and (iii) transport failures, where the object is lifted without dropping but does not reach within 0.1 m of the goal. The results show that transport failures dominate across the six unseen objects, indicating that precise cooperative transport is the primary challenge in this task. Notably, **MAPPO w PI** exhibits a significantly higher grasp-and-lift failure rate than the other methods, likely because it is conditioned on privileged object IDs during training while unseen objects are assigned random IDs. This mismatch can induce inappropriate grasp strategies, highlighting the need for accurate object identification.

Overall, the proposed method generalizes to diverse objects under decentralized execution by reconstructing object-dependent representations from local observations.

### D. RQ3: Can the Trained Policy Successfully Transport Unseen Objects in the Real World?

1) **Setup:** To confirm the effectiveness of DeReCo, we conducted hardware experiments with two HSRs and two unseen objects, as shown in Fig. 6. We compared **DeReCo** with **MAPPO w/o AE**, which is the best-performing baseline in simulation. For each method, we deployed the best policy trained in simulation on the real robots. Each gripper finger was equipped with a GelSight Mini sensor at 60 Hz for contact-force measurement, and an OptiTrack motion-capture system at 120 Hz provided the poses of the robots' end-effectors and the object. The observation and action were similar to those used in simulation. Success is defined as achieving a final object-goal distance error of less than 0.1 m. For fair comparison, the initial positions of the robots and the object were set identically across both methods.

2) **Result:** Table II shows the success rates and final object-goal distance errors over five trials. Both **MAPPO w/o AE** and **DeReCo** achieved grasp-and-lift for both objects in all five trials. However, **MAPPO w/o AE** failed during transport: it did not bring the board within 0.1 m of the goal, and the frame tipped over after lifting, as shown in Fig. 7a. In contrast, **DeReCo** successfully transports both objects, as shown in Fig. 7b, and achieves final object-goal distance errors below 0.1 m on average for both objects.

Overall, the proposed method can successfully transport unseen objects in the real world.

## VI. DISCUSSION

This section introduces the limitations of DeReCo and outline possible directions for future work.

We trained the policies on three representative shapes by randomizing the object mass and friction coefficients within predefined ranges. The proposed method achieves high success rates on unseen objects not included in training. However, extending the diversity of shapes and the ranges of mass and friction can degrade training performance, since extensive domain randomization increases training cost [26]. Scaling to a broader range of shapes and physical properties remains an important direction for future work.

Adapting to different numbers of robots is a crucial direction for future work. This study focuses on generalization

TABLE I: Comparison of success rates on seen and unseen objects. The symbol † indicates that privileged information (PI) was used for seen objects during execution.

Method	Seen Objects				Unseen Objects						
	Bar	Cylinder	Board	Avg.	Hexagon	Triangle	L bar	Thick bar	Octagon	Semi-ellipse	Avg.
MAPPO w/o PI	0.66	0.54	0.90	0.70	0.57	0.50	0.63	0.70	0.57	0.49	0.58
MAPPO w/o PI + LSTM	0.55	0.26	0.46	0.42	0.33	0.39	0.48	0.21	0.30	0.44	0.36
MAPPO w/o AE	0.81	0.69	0.95	0.82	0.72	0.61	0.74	0.72	0.71	0.60	0.68
MAPPO w/o AE + LSTM	0.57	0.35	0.73	0.55	0.38	0.35	0.50	0.36	0.37	0.42	0.40
MAPPO w PI†	0.92	<b>0.83</b>	<b>0.96</b>	<b>0.91</b>	0.44	0.31	0.53	0.60	0.47	0.33	0.45
<b>DeReCo</b>	<b>0.96</b>	<b>0.83</b>	0.94	<b>0.91</b>	<b>0.85</b>	<b>0.70</b>	<b>0.86</b>	<b>0.85</b>	<b>0.86</b>	<b>0.69</b>	<b>0.80</b>

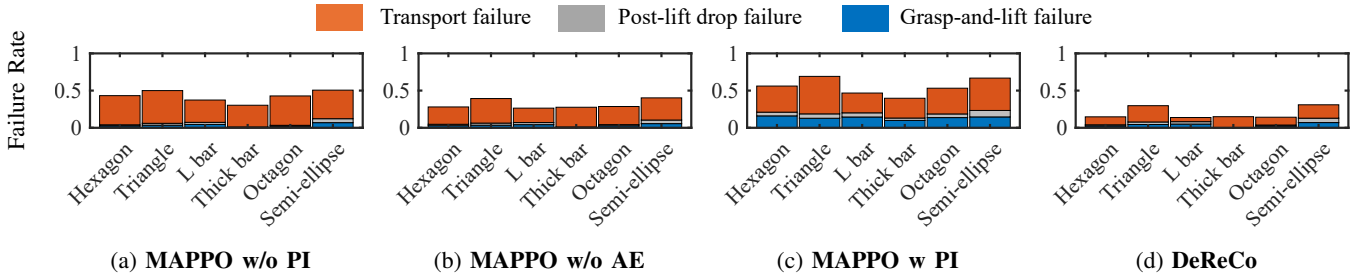


Fig. 5: Failure analysis on unseen objects for four representative methods

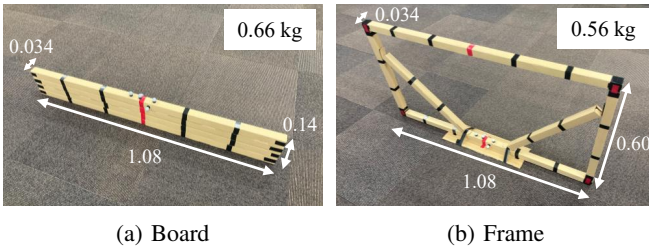


Fig. 6: Objects used in real experiments. All units are meters.

TABLE II: Comparisons of real-robot experiments

Method	Board		Frame	
	Success	Error [m]	Success	Error [m]
MAPPO w/o AE	0/5	0.18 ± 0.06	0/5	0.34 ± 0.00
<b>DeReCo</b>	<b>5/5</b>	<b>0.09 ± 0.01</b>	<b>4/5</b>	<b>0.09 ± 0.01</b>

across object shapes and physical properties in multi-robot cooperative transport with a minimal two-robot setup. Our current approach builds on MAPPO, whose policy input dimensionality depends on the number of robots, limiting its applicability to configurations with a different number of robots. As future work, we will incorporate our approach into decentralized MARL formulations that do not depend on the number of robots, followed by real-robot validation of scalability [6], [7].

## VII. CONCLUSION

This paper proposed DeReCo, a novel MARL framework that decouples representation and coordination learning for object-adaptive multi-robot cooperative transport. DeReCo adopts a three-stage training strategy: (1) centralized coordination learning with privileged object information, (2)

reconstruction of object-dependent representations from local observations, and (3) progressive removal of privileged information for decentralized execution. This decoupling mitigates interference between representation and coordination learning and enables stable and sample-efficient training. Simulation experiments with two HSRs across nine object shapes with varying masses and friction coefficients, including six unseen shapes, show that DeReCo outperforms baseline methods. Real-robot experiments on two unseen objects further confirmed successful sim-to-real transfer.

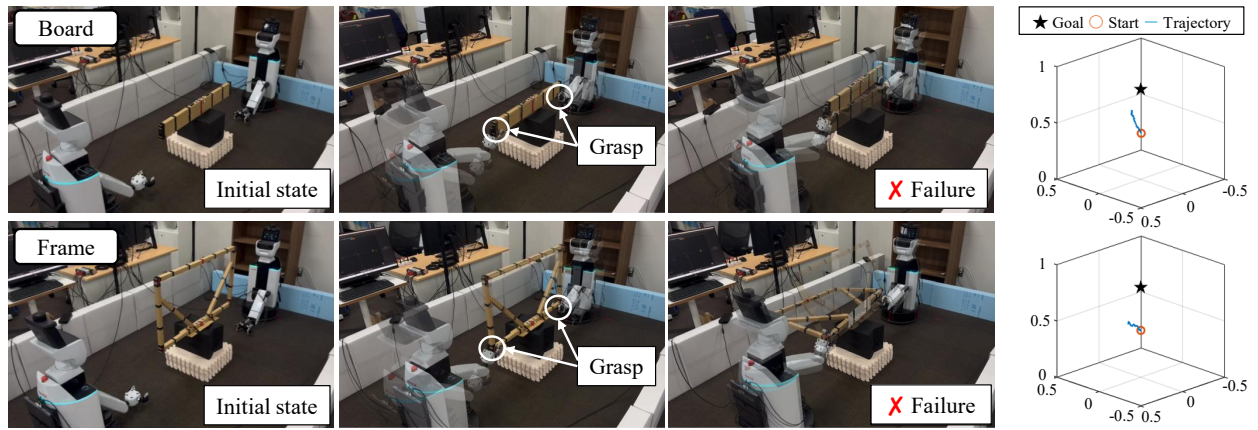
As future work, we plan to extend the proposed method to handle a wider range of object properties while quantitatively evaluating its performance in larger multi-robot teams.

## ACKNOWLEDGMENTS

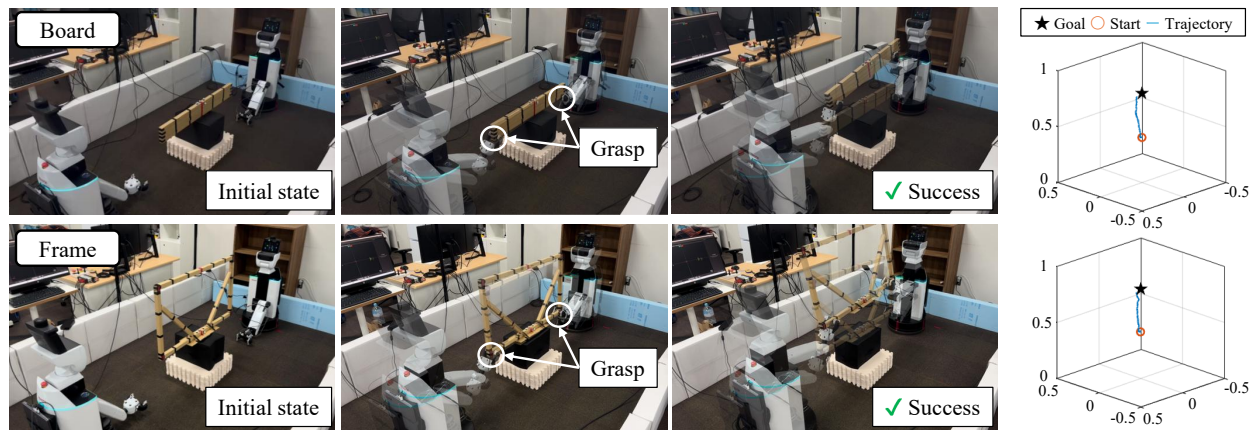
This work was supported by JSPS KAKENHI Grant Number JP25K21315 and the research grant program of The Futaba Foundation.

## REFERENCES

- [1] I.-S. Bernard-Tiong, Y. Tsurumine, R. Sota, K. Shibata, and T. Matsumura, “Cooperative grasping and transportation using multi-agent reinforcement learning with ternary force representation,” in *2025 IEEE/SICE International Symposium on System Integration (SII)*, 2025, pp. 973–978.
- [2] Y. Feng, C. Hong, Y. Niu, S. Liu, Y. Yang, and D. Zhao, “Learning multi-agent loco-manipulation for long-horizon quadrupedal pushing,” in *2025 IEEE International Conference on Robotics and Automation (ICRA)*, 2025, pp. 14 441–14 448.
- [3] B. Pandit, A. Gupta, M. S. Gadde, A. Johnson, A. K. Shrestha, H. Duan, J. Dao, and A. Fern, “Learning decentralized multi-biped control for payload transport,” in *Proceedings of The 8th Conference on Robot Learning*, vol. 270. PMLR, 2025, pp. 1021–1034.
- [4] D. K. Mehta, A. Joglekar, and V. Krovi, “Deep reinforcement learning for coordinated payload transport in biped-wheeled robots,” in *2025 IEEE International Conference on Robotics and Automation (ICRA)*, 2025, pp. 14 992–14 998.



(a) MAPPO w/o AE



(b) DeReCo

Fig. 7: Comparisons of real-robot demonstrations.

- [5] J. Zeng, A. M. Gimenez, E. Vinitzky, J. Alonso-Mora, and S. Sun, "Decentralized aerial manipulation of a cable-suspended load using multi-agent reinforcement learning," in *Proceedings of The 9th Conference on Robot Learning*, vol. 305. PMLR, 2025, pp. 3850–3868.
- [6] K. Shibata, T. Jimbo, and T. Matsubara, "Deep reinforcement learning of event-triggered communication and consensus-based control for distributed cooperative transport," *Robotics and Autonomous Systems*, vol. 159, p. 104307, 2023.
- [7] W.-T. Chen, M. Nguyen, Z. Li, G. N. Sue, and K. Sreenath, "Decentralized navigation of a cable-towed load using quadrupedal robot team via MARL," *arXiv preprint arXiv:2503.18221*, 2025.
- [8] R. Lowe, Y. WU, A. Tamar, J. Harb, O. Pieter Abbeel, and I. Mordatch, "Multi-agent actor-critic for mixed cooperative-competitive environments," in *Advances in Neural Information Processing Systems*, vol. 30, 2017.
- [9] J. Hu, W. Liu, H. Zhang, J. Yi, and Z. Xiong, "Multi-robot object transport motion planning with a deformable sheet," *IEEE Robotics and Automation Letters*, vol. 7, no. 4, pp. 9350–9357, 2022.
- [10] D. Koung, O. Kermorgant, I. Fantoni, and L. Belouaer, "Cooperative multi-robot object transportation system based on hierarchical quadratic programming," *IEEE Robotics and Automation Letters*, vol. 6, no. 4, pp. 6466–6472, 2021.
- [11] F. Kennel-Maushart and S. Coros, "Payload-aware trajectory optimisation for non-holonomic mobile multi-robot manipulation with tip-over avoidance," *IEEE Robotics and Automation Letters*, vol. 9, no. 9, pp. 7669–7676, 2024.
- [12] G. Li and G. Loianno, "Nonlinear model predictive control for cooperative transportation and manipulation of cable suspended payloads with multiple quadrotors," in *2023 IEEE/RSJ International Conference on Intelligent Robots and Systems (IROS)*, 2023, pp. 5034–5041.
- [13] S. Sun, X. Wang, D. Sanalitra, A. Franchi, M. Tognon, and J. Alonso-Mora, "Agile and cooperative aerial manipulation of a cable-suspended load," *Science Robotics*, vol. 10, no. 107, p. eadu8015, 2025.
- [14] R. T. Fawcett, L. Amanzadeh, J. Kim, A. D. Ames, and K. A. Hamed, "Distributed data-driven predictive control for multi-agent collaborative legged locomotion," in *2023 IEEE International Conference on Robotics and Automation (ICRA)*, 2023, pp. 9924–9930.
- [15] N. De Carli, R. Belletti, E. Buzzurro, A. Testa, G. Notarstefano, and M. Tognon, "Distributed NMPC for cooperative aerial manipulation of cable-suspended loads," *IEEE Robotics and Automation Letters*, vol. 10, no. 10, pp. 10546–10553, 2025.
- [16] P. Culbertson, J.-J. Slotine, and M. Schwager, "Decentralized adaptive control for collaborative manipulation of rigid bodies," *IEEE Transactions on Robotics*, vol. 37, no. 6, pp. 1906–1920, 2021.
- [17] L. Yan, T. Stouraitis, and S. Vijayakumar, "Decentralized ability-aware adaptive control for multi-robot collaborative manipulation," *IEEE Robotics and Automation Letters*, vol. 6, no. 2, pp. 2311–2318, 2021.
- [18] M. Sombolstan and Q. Nguyen, "Hierarchical adaptive control for collaborative manipulation of a rigid object by quadrupedal robots," in *2023 IEEE/RSJ International Conference on Intelligent Robots and Systems (IROS)*, 2023, pp. 2752–2759.
- [19] X. B. Peng, M. Andrychowicz, W. Zaremba, and P. Abbeel, "Sim-to-real transfer of robotic control with dynamics randomization," in *2018 IEEE International Conference on Robotics and Automation (ICRA)*, 2018, pp. 3803–3810.
- [20] Z. Xu, W. Yu, A. Herzog, W. Lu, C. Fu, M. Tomizuka, Y. Bai, C. K. Liu, and D. Ho, "COCO: Contact-aware online context inference for generalizable non-planar pushing," in *2021 IEEE/RSJ International Conference on Intelligent Robots and Systems (IROS)*, 2021, pp. 176–182.
- [21] I. Dadiotis, M. Mittal, N. Tsagarakis, and M. Hutter, "Dynamic object goal pushing with mobile manipulators through model-free constrained

- reinforcement learning,” in *2025 IEEE International Conference on Robotics and Automation (ICRA)*, 2025, pp. 13 363–13 369.
- [22] S. Jeon, M. Jung, S. Choi, B. Kim, and J. Hwangbo, “Learning whole-body manipulation for quadrupedal robot,” *IEEE Robotics and Automation Letters*, vol. 9, no. 1, pp. 699–706, 2024.
- [23] F. A. Oliehoek and C. Amato, *A Concise Introduction to Decentralized POMDPs*, 1st ed. Springer Publishing Company, Incorporated, 2016.
- [24] C. Yu, A. Velu, E. Vinitzky, J. Gao, Y. Wang, A. Bayen, and Y. Wu, “The surprising effectiveness of PPO in cooperative multi-agent games,” in *Advances in Neural Information Processing Systems*, vol. 35, 2022, pp. 24 611–24 624.
- [25] J. Schulman, F. Wolski, P. Dhariwal, A. Radford, and O. Klimov, “Proximal policy optimization algorithms,” *arXiv preprint arXiv:1707.06347*, 2017.
- [26] G. Tiboni, P. Klink, J. Peters, T. Tommasi, C. D’Eramo, and G. Chaltatzaki, “Domain randomization via entropy maximization,” in *The Twelfth International Conference on Learning Representations*, 2024.